Chapter 5

Optical reflection from defect lattices

5.1 Introduction

In the previous chapters we considered the elastic and hydrodynamic properties of defects and defect lattices. A study of optical reflection from defect lattices often gives an insight into their structures. Also the structure in turn can give rise to interesting optical effects which may not exist in other systems. The main feature of a liquid crystal is that it is optically birefringent. The refractive index tensor should confirm to the symmetry of the liquid crystalline systems. In nematic, cholesteric and smectic A liquid crystals two of the three diagonal components of the index tensor are identical. In other words, the tensor surface can be visualised as an uniaxial ellipsoid of revolution about n. On the other hand a smectic C liquid crystal is biaxial with all three principal components different. The tensor surface here, is a triaxial ellipsoid. This unique feature of refractive index anisotropy can be contrasted with that of an isotropic system

where the refractive index is a scalar and the corresponding tensor surface is a sphere. The refractive index anisotropy and the director orientation gives rise to interesting polarisation dependant optical phenomena. The study of these features is carried out under the restrictive assumption that the structure under study is not affected by the optical fields which is a reasonable assumption to make at low intensities of the incident field.

We study optics in two important modes viz., a) the reflection mode and **2)** the diffraction mode. We consider in this and the next two chapters the optics of two defect lattices viz., twist grain boundary smectics (TGBS) and solitons with tapered lattices. We are interested in TGBS since it is rather similar to a multisoliton lattice like the cholesteric soliton lattice. Optics of such multisoliton lattices have already been considered by others. In this context, it is relevent to summarise the main results of reflection and diffraction studies on a soliton lattice of a cholesteric. The lattice has nematic like nearly uniform regions followed by a soliton of a twist. The important optical features are [1]

- Many reflection bands exist even at normal incidence. Each band has a finer structure with three sub-bands with different polarisation features. The central band is polarisation insensitive and the side bands reflect orthogonal polarisation states.

- Diffraction pattern is very sensitive to sample thickness and the intial polarisation state of the electric vector.

- Diffraction from absorbing soliton lattice can be used to elucidate the structure.

We may expect some of these features to be present in this study of defect lattices viz., TGBS and tapered lattice. In addition we can expect some unusual optical effects since they are structurally very different in detail. It is important to remark that tapered lattices are dynamic in nature propagating with a finite velocity. Here we have considered them at such low velocities that, from the point of view of optics they are static structures. Relaxing this constraint will lead to doppler shift in the frequencies of reflected and diffracted light.

5.2 Theory of Reflection and Transmission

We have worked out the optical reflection and transmission properties using the Berreman's 4 x 4 matrix formulation [2] of Maxwell's equations. Here the heterogenous anisotropic medium is divided into thin homogenous slabs, in each of which Maxwell's equations are solved. In any given slab

$$\frac{\partial \psi(z)}{\partial z} = \frac{i\omega}{c}\Delta(z)\psi(z) \tag{5.1}$$

where

$$\psi(z) = \begin{pmatrix} E_x \\ H_y \\ E_y \\ -H_x \end{pmatrix}$$

and $\Delta(z)$ is a 4 × 4 matrix whose elements contain the dielectric tensor components which are periodic in z. In our case it is periodic along the z-

direction and is of the form

$$\begin{pmatrix} 0 & 1 - X^2/\varepsilon_3 & 0 & 0 \\ \varepsilon + \delta\cos 2qz & 0 & \delta\sin 2qz & 0 \\ 0 & 0 & 0 & 1 \\ \delta\sin 2qz & 0 & \varepsilon - X^2 - \delta - X^2 - \delta\cos 2qz & 0 \end{pmatrix}$$

Here $X = (2\pi/\lambda)\sqrt{\epsilon_0}\theta_i$ with θ_i = angle of incidence with respect to the pitch and ε_0 = dielectric constant of the incident medium. $\varepsilon = (\varepsilon_1 + \varepsilon_2)/2$

$\delta = (\varepsilon_1 - \varepsilon_2)/2$

$q = 2\pi/P$ and P = pitch of the periodic structure. Here E_x, E_y and H_x, H_y are respectively the components of the electric and magnetic fields in a plane perpendicular to the twist axis. Integrating (*5.1)* we get

$$\psi(z) = M\psi(0) \tag{5.2}$$

The matrix M, called the propagation matrix, relates the field components in the $(j+1)^{th}$ slab to those in the j^{th} slab. The eigenvectors of M give the modes which travel unaltered inside the medium. The reflection and transmission coeffiecients are calculated from this as follows. The electric and magnetic field components of $\psi(0)$ is made up of two parts, the incident and the reflected part.

$$\psi(0) = \psi_i + \psi_r \tag{5.3}$$

The field components after j slabs consists of only the transmitted part.

$$\psi(z) = \psi_t \tag{5.4}$$

For a plane wave of frequency w, incident at an angle θ_1 to the layer normal

of the first layer, of refractive index n_1, the incident part can be written as

$$\psi_i = \begin{pmatrix} E_x \\ r_x E_x \\ E_y \\ r_y E_y \end{pmatrix} \tag{5.5}$$

where T, $= \frac{n_1}{\cos\theta_1}$ T, $= n_1 \cos\theta_1$ The reflected and Transmitted waves are

$$\psi_r = \begin{pmatrix} R_x \\ -r_x R_x \\ R_y \\ -r_y R_y \end{pmatrix} \tag{5.6}$$

$$\psi_t = \begin{pmatrix} T_x \\ r_{x\prime} T_x \\ T_y \\ r_{y\prime} T_y \end{pmatrix} \tag{5.7}$$

where $r_{x\prime} = \frac{n_2}{\cos\theta_2}, r_{y\prime} = \frac{n_2}{\cos\theta_2}$ n_2 = refractive index of the second medium $\theta_2 = \sin^{-1}(\frac{n_1}{n_2}\sin\theta_1)$ From equation (5.2) and from the knowledge of polarisation state and the amplitude of the incident wave, we can get the reflected and transmitted coefficients namely, R,, R_y, T_x and T_y.

This method can be used to calculate the reflection spectrum, the transmission spectrum and the phase of the transmitted wave. It must be emphasised that in actual experiments we also have the bounding isotropic media. Then we use the method of Galatalo et. al [3], to calculate the eigenmodes which travel unchanged both in the liquid crystal and in the bounding media. This method consists of writing the proper modes of the multilayer heterogenous media in terms of the modes in the bounding isotropic media in the form of 2 x 2 matrices.

5.3 Twist grain boundary smectics

The structures of TGBS have been established to a certain degree by X-ray studies [4]. From these studies, it has become clear that the TGBS are a helical stack of smectic blocks with the smectic layer normal perpendicular to the twist axis. Any two neighbouring smectic blocks are connected through a twist grain boundary. Here also, as in crystals [5] the twist grain boundary is a periodic array of screw dislocations. The TGBS are classified as commensurate or incommensurate, depending upon whether or not the net director rotation across the grain is a rational multiple of 2π. In the case of commensurate TGBS, the twist axis also happens to be a N-fold screw axis, N being an integer. On the other hand, the incommensurate structures have no such screw symmetry. Further the smectic blocks could be of smetic A (S_A), smectic C (S_C) or smectic C^* (S_{C^*}) structure. Then the TGBS are respectively designated as TGB_A, TGB_C and TGB_{C^*}. Optical studies on TGBS structures have been largely confined to the determination of their pitch and the sense of the helix. Even here it has been tacitly assumed that these are akin to cholesteric liquid crystals [6], [7]. Interestingly, we find that these liquid crystals are, optically, different from cholesterics and S_{C^*}.

5.3.1 Model

The model of TGBS which we have used in our calculations is shown schematically in Figure 5.1. Optically the smectic blocks can be thought of as thick birefringent plates which are arranged in a uniform helical stack. Any two such neighbouring smectic blocks are connected by a grain boundary. In our model

the grain boundary is approximated by a stack of thin birefringent plates. These thin plates smoothly rotate and connect the adjacent smectic blocks. Generally the size of the smectic block is of the order 1000 $A°$ and that of the grain boundary is about 150 $A°$. The director orientation profile in such a model

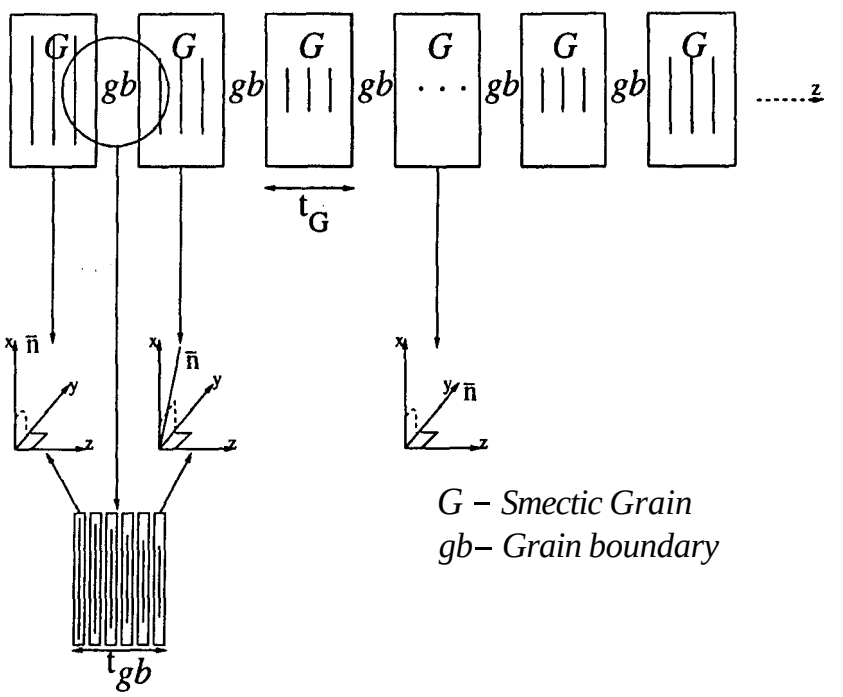

Figure 5.1: *Schematic representation of the TGB_A model. The line inside each block is the projection of director n on x axis.*

is as shown in Figure 5.2. It is rather similar to the cholesteric twist soliton lattice since it has uniform regions seperated by twisted regions of the grain boundaries. The important differences are (i) the uniform regions globally twist as we go from one uniform region to the next and (ii) the twist in the grain boundary is small compared to the π twist of cholesteric soliton lattice. As a further approximation to this model, we have also considered the case

where the grain boundary is ignored altogether. Also, we must note that in

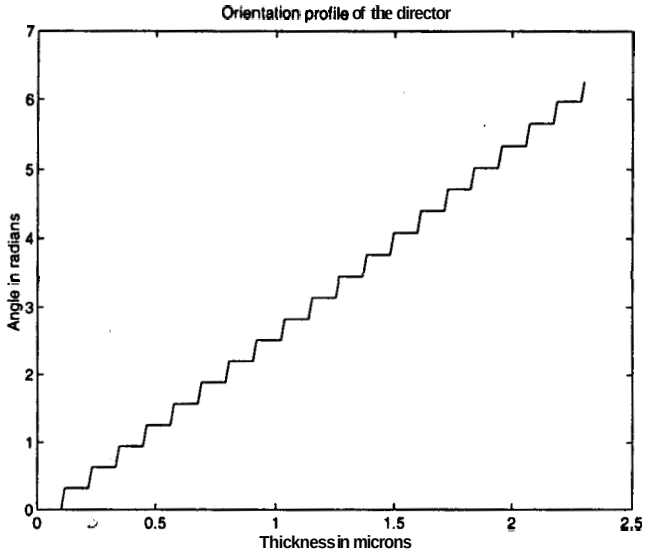

Figure 5.2: *Director orientation profile of* TGB_A *model.*

TGB_A the blocks have uniaxial symmetry while in TGB_C the blocks are biaxial since S_C is of monoclinic symmetry. In the twist grain boundaries of both TGB_A and TGB_C we can assume, to a good approximation, local uniaxial symmetry. As a result of this both in the smectic blocks and the grain boundaries of TGB_A the index and absorption tensors are ellipsoids of revolution about the local director. On the other hand in TGB_C, in the smectic blocks the index and absorption tensors are triaxial ellipsoids. In these ellipsoids one of their principal axes will be along the local 2-fold axis of smectic C blocks and the other two will be at an angle with respect to one another. However, in the grain boundary of TGB_C the two tensors become ellipsoids of revolution about the local director. Further, in the smectic blocks of TGB_c we consider two geometries where in the local two-fold axis of smectic blocks is either par-

allel or perpendicular to the twist axis. These are respectively designated as $TGB_{C_{\parallel}}$ and $TGB_{C_{\perp}}$. In $TGB_{C_{\parallel}}$, the molecules are perpendicular to the twist axis in the smectic blocks and in $TGB_{C_{\perp}}$ they spiral at a constant angle about the twist axis.

5.3.2 Reflection and Transmission Spectra

Normal Incidence

(a) Reflection spectra:

We find that a total reflection occurs at $\lambda = \mu p$ with p being the pitch of the structure and μ being its mean refractive index. This Bragg reflection has many features in common with the Bragg band seen in the cholesterics [8]. For example, a circularly polarized light of the same sense as that of the structure is totally reflected. The width of the reflection band is $p\delta\mu$ with $\delta\mu$ being the layer birefringence. Also the standing electromagnetic wave inside the reflection band has, locally, a linear polarization state. But unlike in cholesterics, the local electric vector of the standing wave does not follow the equivalent of the cholesteric director viz, the smectic layer normal. However, globally the linear state rotates uniformly about the twist axis. As in a cholesteric soliton lattice we get many reflection bands and the wavelengths at which they occur are decided by the symmetry of the screw axis. They occur at $\lambda = \mu p/m$ for $2, 4, 6...$ (N is even) screw symmetry and at $\lambda = 2\mu p/m$ for $1, 3, 5...$ (N is odd) screw symmetry, m being an integer. We can understand on a simple model, the positions and polarization features of the prominent reflections. A left handed structure of N-fold screw axis and of pitch p

can also be looked upon as a right handed structure with a N'-fold screw axis with a pitch p'. Therefore, we can get from the same structure both right circularly polarized and left circularly polarized reflections. In the case of N = 4,however, both left and right have the same N-fold screw symmetry and hence in all the reflection bands this structure reflects both right circular and left circular polarizations. The positions of the interference maxima can be worked out by the so called kinematical theory of reflection from a helical stack of birefringent plates [9]. This procedure is also implied in the work of Joly et al concerning a helical stack of thick birefringent plates [10]. However, this method predicts only the positions at which reflection peak of a particular polarization occurs. For a knowledge of tlic intensity of reflections and the width of reflection bands, a theory taking into account multiple reflections is necessary. The theory presented in the previous section incorporates this feature explicitly. A few computed reflection spectra are shown in Figure 5.3. We notice that neither reflections permitted for all values of m are seen nor the intensities of the different reflections are the same. As stated earlier, important feature of these reflections is that in some of them circularly polarized light of the same sense as that of the helix is strongly reflected and in some others circularly polarized light of the opposite sense is strongly reflected. In view of this, the determination of the pitch and the sense of the helix could be completely wrong if we happen to treat any of these higher order reflections as a cholesteric reflection.

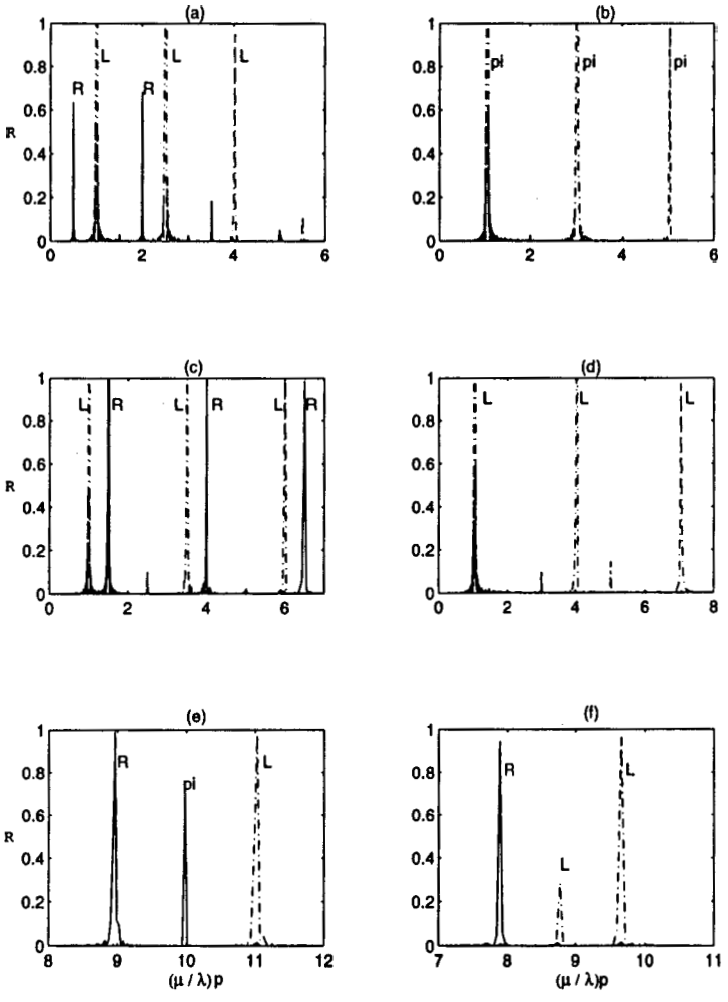

Figure 5.3: *The reflectance (R) as a function of $(\mu p/\lambda)$ smectic block thickness = 1000 A°. (a) N = 3, (b) N = 4, (c) N = 5, (d) N = 6, (e) N = 20 and (f) Incommensurate TGB_A with an inter-grain angle of nearly* 18" *and here p denotes the pitch of the nearest commensurate structure of inter-grain angle of* 18° *exact. Here R and L represent respectively the right and left circularly polarized state and pi represents the polarization insensitive reflection. Our computations are for a left handed structure.*

(b) Incommensurate structures

If the structure is incommensurate the spectrum gets considerably altered. In Figure 5.3(f), we give the higher order reflection spectrum for

an inter-grain twist of nearly 18°. In fact the inter-grain twist is $2\pi\alpha$, a being an irrational number close to 0.05. This spectrum is quite different from that shown in Figure 5.3(e) which corresponds to a commensurate TGB with an inter-grain angle of exactly 18°. We note that the reflections do not any more occur exactly at $\lambda = \mu p/m$. Also, interestingly in this example, the polarization insensitive band is absent.

(c) Anomalous optical rotation

As in cholesterics here also the base states are right and left circular polarizations travelling with different velocities. Hence the structure has optical rotation. As one approaches a band of either left or right circular

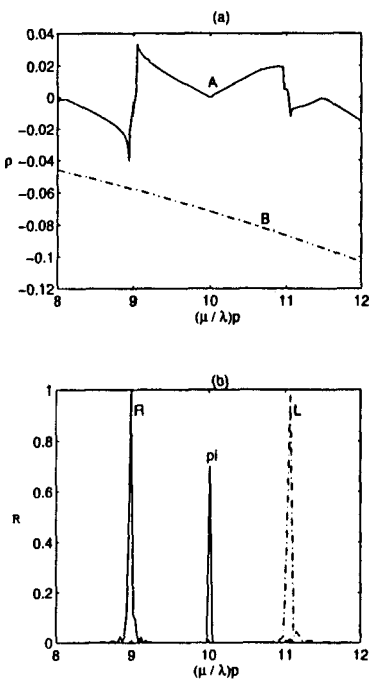

Figure 5.4: *(a) Rotatory power (ρ) as a function of $(\mu p/\lambda)$. Here A is for TGB_A and B is for a cholesteric with same parameters but using de Vries formula. (b) Higher order rejection spectrum of TGB_A in the same $(\mu p/\lambda)$ range.*

reflection, the optical rotatory power obtained from the phase difference between right and left emergent states increases and changes sign on crossing the band i. e. , the rotation becomes anomalous. The rotation anomaly in a band associated with the reflection of right circularly polarized light is opposite in sign to that found in a band associated with the reflection of left circularly polarized light. Also we find that the rotatory power in the low wavelength range of the main reflection band at $\mu p/\lambda = 1$ does not obey the de Vries formula valid for $\lambda << \mu P$ for cholesterics [11]. It may be noticed that the difference is both in sign and in magnitude. All these features are depicted in Figure 5.4. Hence even a study of optical rotation cannot lead to an unambiguous determination of pitch or helical sense.

(d) Effect of structural parameters

It is theoretically established that the smectic order parameter which is constant in a smectic block gradually decreases and finally vanishes at the centre of the grain boundary. As a result of this the director twist in the grain boundary will be non-uniform. Lubensky and Renn predict a gaussian variation of the order parameter. Using this fact and a simple model we calculated the non-uniform director twist. Optical calculations based on this model were compared with those carried out on a less realistic model where we assume a uniform director twist in the grain boundary. For all practical purposes the model, with grain boundaries of uniform twist, appeared good enough. In our simplified model the total twist in the grain boundary is comparable to that in a normal cholesteric of an equivalent thickness. (i.e., its pitch is about

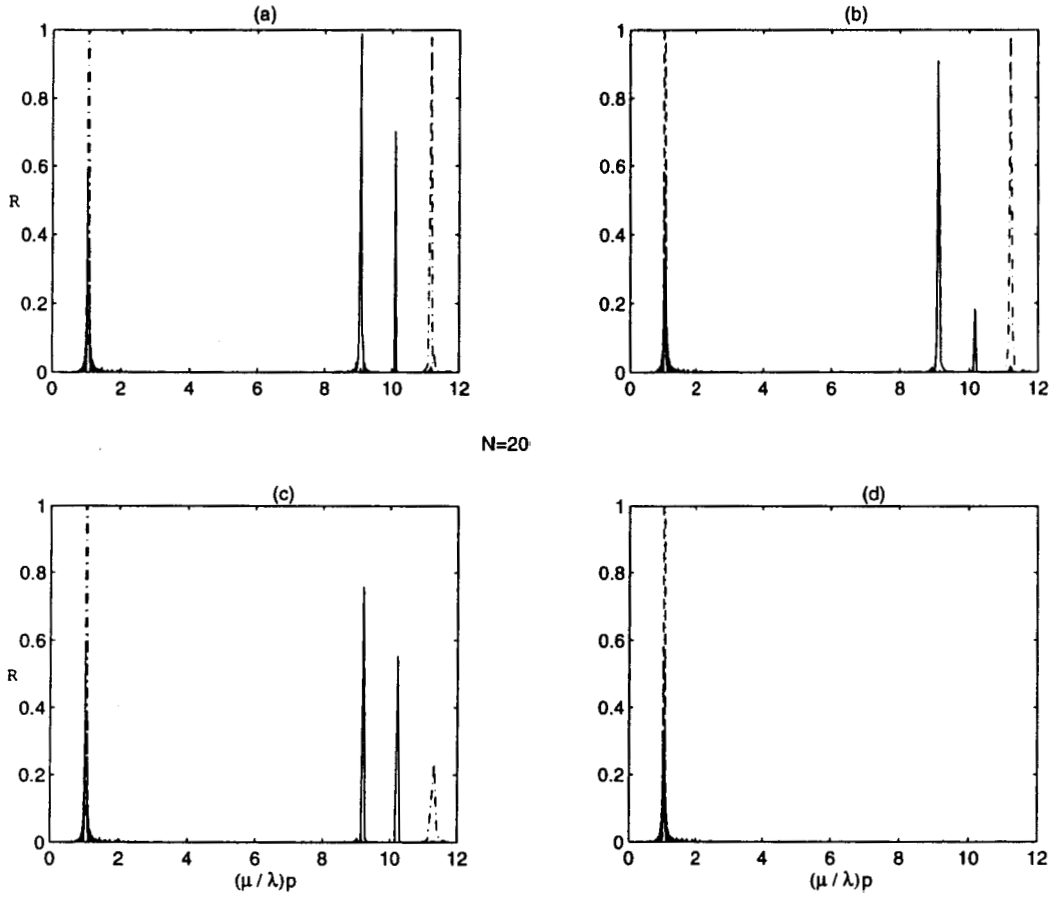

Figure *5.5: Rejection spectra of* TGB_A *with* $N = 20$ *for a grain boundary thickness of 150* $A°$ *and for different thicknesses of the smectic block (a) 750* $A°$ *(b) 500* A^o *(c) 300* A^o *and (d)* $100\ A^o$

0.3 microns or more). We now consider the influence of the thickness of the smectic block. In Figure *5.5* we give the reflection spectra for a TGB_A (or $TGB_{C_{||}}$) with an inter-grain angle of $18°$ ($N = 20$) computed for different thickness of the smectic block keeping the grain boundary thickness the same. We find that when the smectic block thickness is less than or about the grain boundary thickness, in this case *150* $A°$, the spectrum goes over to that of a cholesteric i. e. , only one reflection band

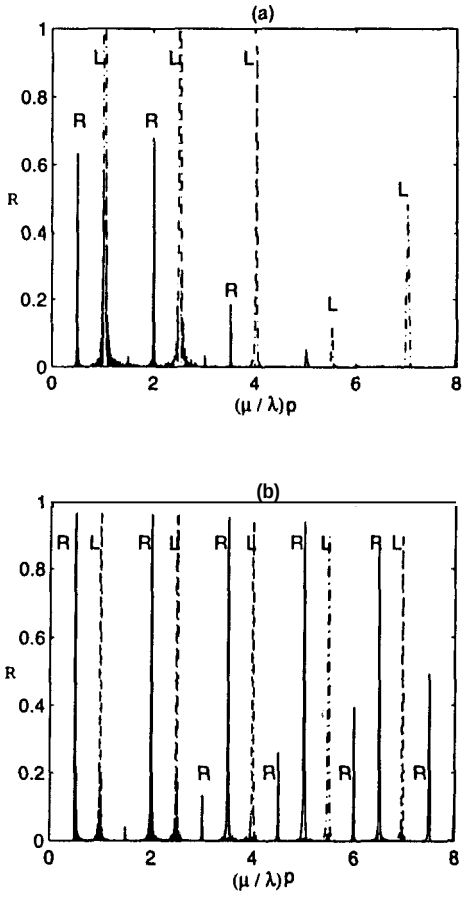

Figure 5.6: *Reflection spectra of TGB_A for $N = 3$, (a) with the grain boundary (b) without the grain boundary.*

at $\mu P/\lambda = 1$. Similarly in the case of $TGB_{C_\perp}$ the spectrum goes over to that of S_{C^*} of a high tilt angle. This effect is true for only small intergrain angles irrespective of the value of N. We have also considered a simplified model of $TGBS$ where we ignore its grain boundaries. We find that this model gives a very different reflection spectrum for intergrain angle greater than or equal to 90°. In Figure 5.6 this difference has been brought out for a TGB_A of a 3-fold screw symmetry. In this context it may be mentioned that Joly and Isaret [10] have studied, using a 2 x 2

matrix formulation the reflection spectra for helical stacks of birefringent plates of very high phase retardation. Some of the features of the *T G B S*

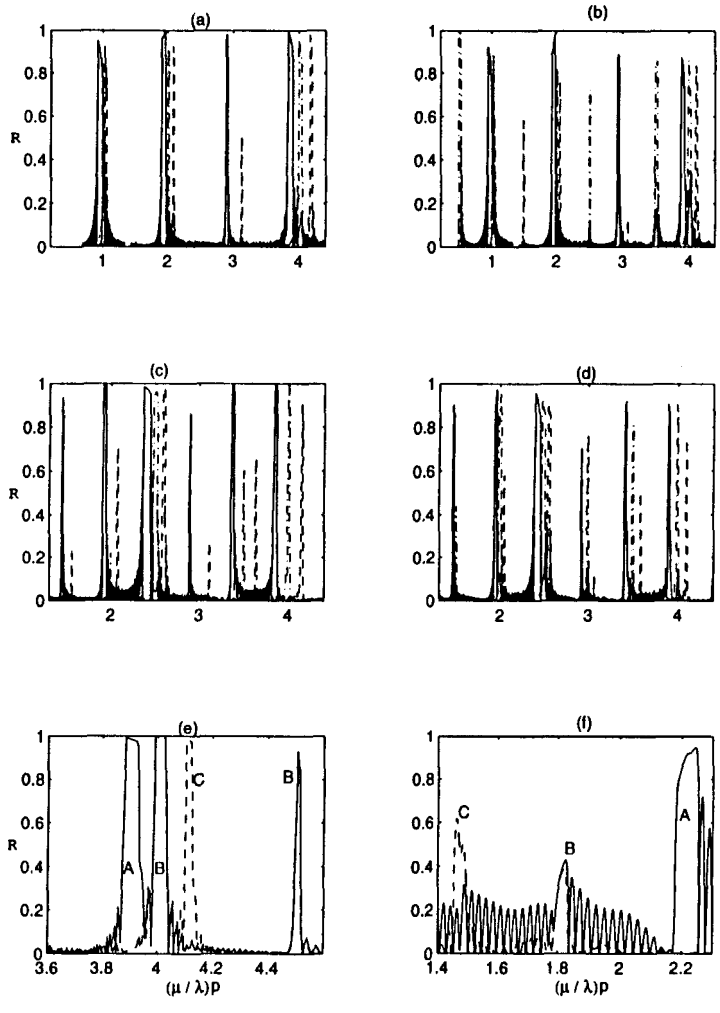

Figure 5.7: *Reflection spectra at an angle of incidence of* 60°. *(a) Reflection peaks occur at integral values of* $(\mu p/\lambda)$ *for* TGB_A *with* $N = 6$, *(b) Reflection peaks occur at integral and half integral values of* $(\mu p/\lambda)$ *for a* $TGB_{C_\perp}$ *with* $N = 6$. *Reflection spectrum of (c)* TGB_A *and (d)* $TGB_{C_\perp}$ *for* $N = 3$ *have half integral reflections in both. Polarization features of a rejection band of (e)* $TGB_{C_\perp}$ *with* $N = 6$ *and (f)* S_{C^*}. *A represents incident T E state reflected as a T E state, B represents incident T E or T M state reflected as a T M or T E state and C represents incident T M state reflected as T M state.*

are present in their systems.

Oblique Incidence

In this geometry also the reflection spectrum is decided by the screw symmetry. In the case of $2, 4, 6...$ (even N) screw symmetry both for TGB_A and $TGB_{C_{||}}$, reflection peaks occur at $\mu p/\lambda = \mathrm{m}$ while for $TGB_{C_\perp}$ they occur at $\mu p/\lambda = m/2$. In Figure 5.7(a) we give the spectrum computed for TGB_A and in Figure 5.7(b) that for $TGB_{C_\perp}$. However for $1, 3, 5...$ (odd N) screw symmetry, the three TGBs, namely TGB_A, $TGB_{C_{||}}$ and $TGB_{C_\perp}$ have reflections at $\mu p/\lambda = m/2$. This is shown in Figure 5.7(c) for TGB_A and in Figure 5.7(d) for $TGB_{C_\perp}$.

As in the case of normal incidence, here also reflections at all permitted values of m are not present. Also, in TGB_A or $TGB_{C_{||}}$ for even or odd values of N and in $TGB_{C_\perp}$ for odd values of N, for angles of incidence greater than about 30° each Bragg band splits up into three sub-bands with different polarization properties. We find that in the lower wavelength sub-band an incident wave with its electric vector perpendicular to the plane of incidence (TE) gets reflected in the same state(TE). On the other hand in the longer wavelength sub-band a wave with its electric vector parallel to the plane of incidence(TM) gets reflected in the same state(TM). In the central sub-band a wave in the TM state gets reflected in the TE state and vice versa. This is explicitly shown in Figure 5.7(e) for one such band. On the other hand, surprisingly for $TGB_{C_\perp}$ for even values of N, we get new reflections at oblique incidence corresponding to half integral values of $\mu p/\lambda$ and they do not split into sub-bands. And in such bands, an incident TE state is reflected as a TM state and vice-versa. One such band is also shown in Figure 5.7(e). Interestingly the polarization features of the three sub-bands shown in Figure 5.7(e) are

rather similar to those found in cholesterics and are quite different from those of normal S_{C^*}. We have shown in Figure 5.7(f) a typical S_{C^*} reflection. This difference is due to the fact that in all the three $TGBs$ considered here, the molecular tilt with respect to the twist axis is quite large. Thus this structure has optical properties that were predicted by Oldano [12] for a S_{C^*} with a tilt angle above a certain value θ_c. As was first shown by him, a S_{C^*} with a tilt angle greater than θ_c is optically different from an S_{C^*} with a tilt angle less than θ_c , in that the short wavelength and long wavelength sub-bands have opposite polarization features in the two cases. In conclusion we notice that oblique reflection studies can distinguish between $TGB_{C_\perp}$ and TGB_A or $TGB_{C_\parallel}$.

5.4 Tapered lattice

In the last chapter, we obtained as a permitted solution, a dynamic soliton state in nematics and ferronematics, with a tapered lattice characterised by a periodic distortion. A typical structure of such a soliton with its tapered lattice is shown in Figure 5.8. The amplitude of the periodic distortion accompanying the soliton decreases exponentially. The period of the distortion also varies from one end of the structure to the other.

In this section, we are interested in the peculiar optical features this structure gives rise to, in the reflection mode. Since the soliton associated with the periodic distortion could either be a twist soliton or a splay-bend soliton we have considered both the cases. The director pattern in these are schematically shown in Figure 5.9. We first consider an ideal tapered lattice where the period

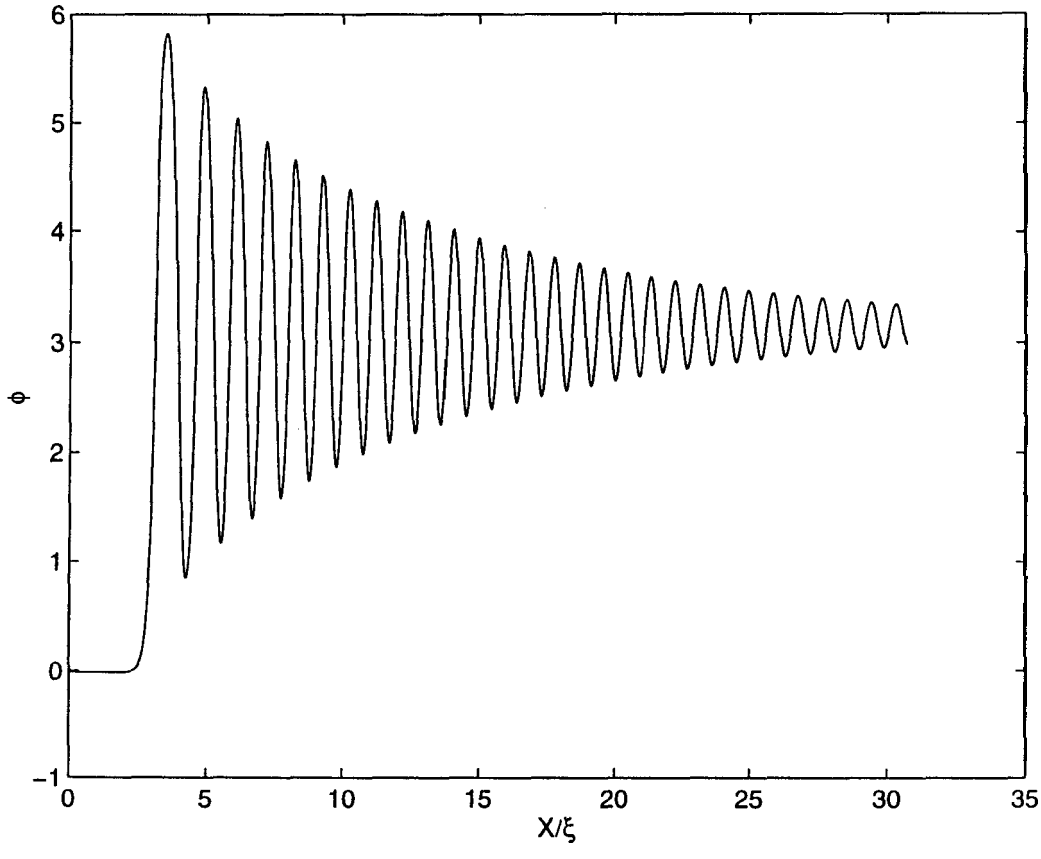

Figure 5.8: *A tapered lattice with* $F/f = -1$ *and* $H = 7000 Gauss$

is a constant all through but the amplitude decays exponentially. Towards the end, we comment on the modifications due to relaxing this constraint of constant period.

5.4.1 Twist-tapered lattice

Bragg reflection at normal incidence

Bragg reflections from a twist tapered lattice at normal incidence can be calculated using the 4 × 4 matrix formulation of the Maxwell's equation discussed earlier. The reflection coefficient (R) for the incident light with a circu-

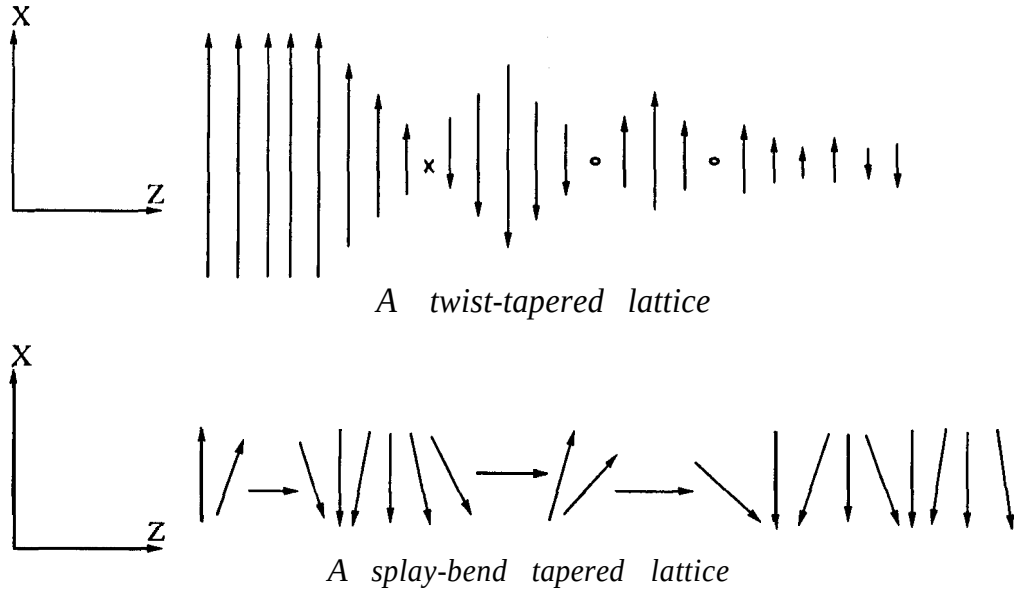

Figure 5.9: *Schematic representation of a twist tapered lattice and a splay-bend tapered lattice*

lar polarisation, has been calculated. As in the case of TGBS, here also there are many reflection bands at normal incidence. Reflections occur at both integral and half-integral values of $\mu p/\lambda$. All the reflection bands reflect both left circularly polarised light and right circularly polarised light. This is not surprising as the structure itself can be looked upon as an alternating stack of left handed twisted structure and a right handed twisted structure of decreasing twist connected by very thin regions of uniform director orientation. **A** typical reflection spectrum is shown in Figure 5.10. We notice the following important features:

- Reflections of both left circular and right circular light have generally noticeably different amplitudes in bands with integral values of $\mu p/\lambda$. In

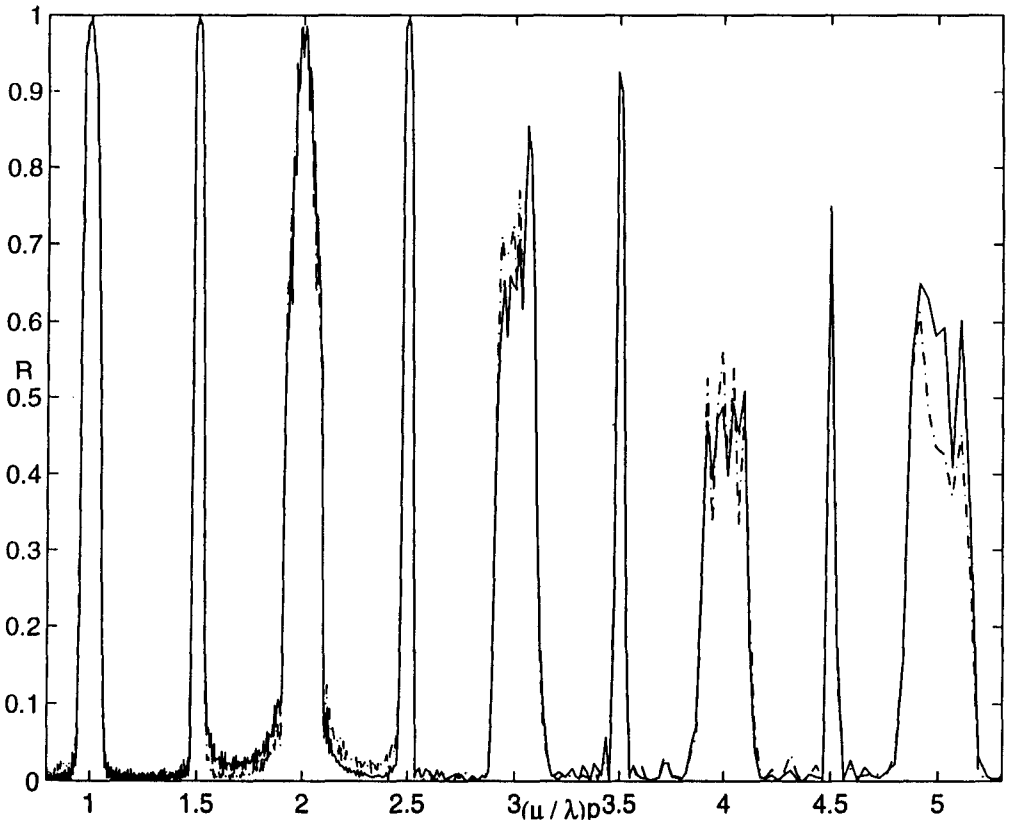

Figure 5.10: *Optical reflection in a twist tapered lattice. Reflection coffiecient for incidence of left circularly polarised light (–) and right circularly polarised light (. – .–). The soliton starts with a left handed twist. The period of the structure is 0.4 microns.*

some of these reflection bands right circular polarisation is reflected more than the left and in some others, left circular polarisation is reflected more than the right.

- All the bands evidently reflect linearly polarised light also. The incident linear polarisation can either be polarised along X axis or along Y axis (see Figure 5.9) called the X polarisation and the Y polarisation respectively. Both X and Y polarisation are reflected in all the bands.

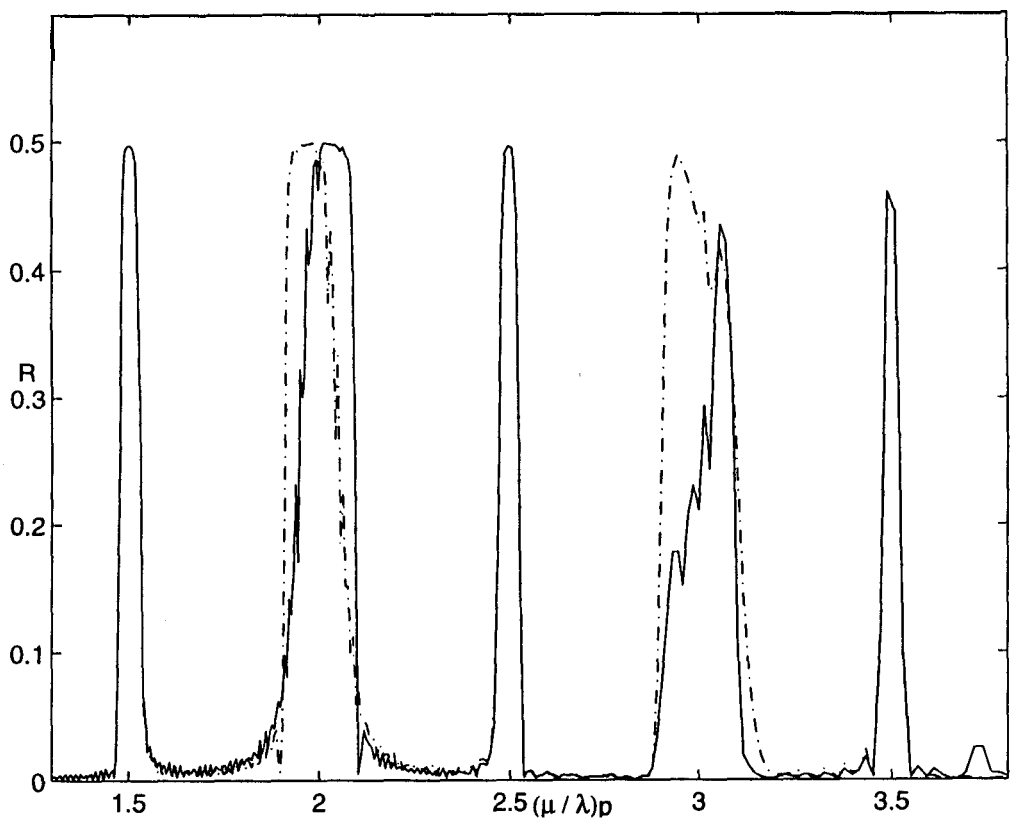

Figure 5.11: *The reflection of X and Y polarisations from the twist tapered lattice showing the shift in reflection peaks. Continuous line is for X polarisation and dashed line is for Y polarisation.*

The computed spectra is shown in Figure 5.11. Interestingly, in every band with integral values of $\mu p/\lambda$, the X polarisation peaks at the shorter wavelength edge of the band and the Y polarisation peaks at the long wavelength edge. But such differences are not seen in bands with half-integral values of $\mu p/\lambda$.

- The structure of the tapered lattice is asymmetric. Hence the reflection coefficient for light incident at $\phi = 0$ end $(R(\mathrm{k}))$ need not be identical to reflection coeffiecient for light incident at $\phi \approx \pi$ $(R(-\mathrm{k}))$. Surprisingly,

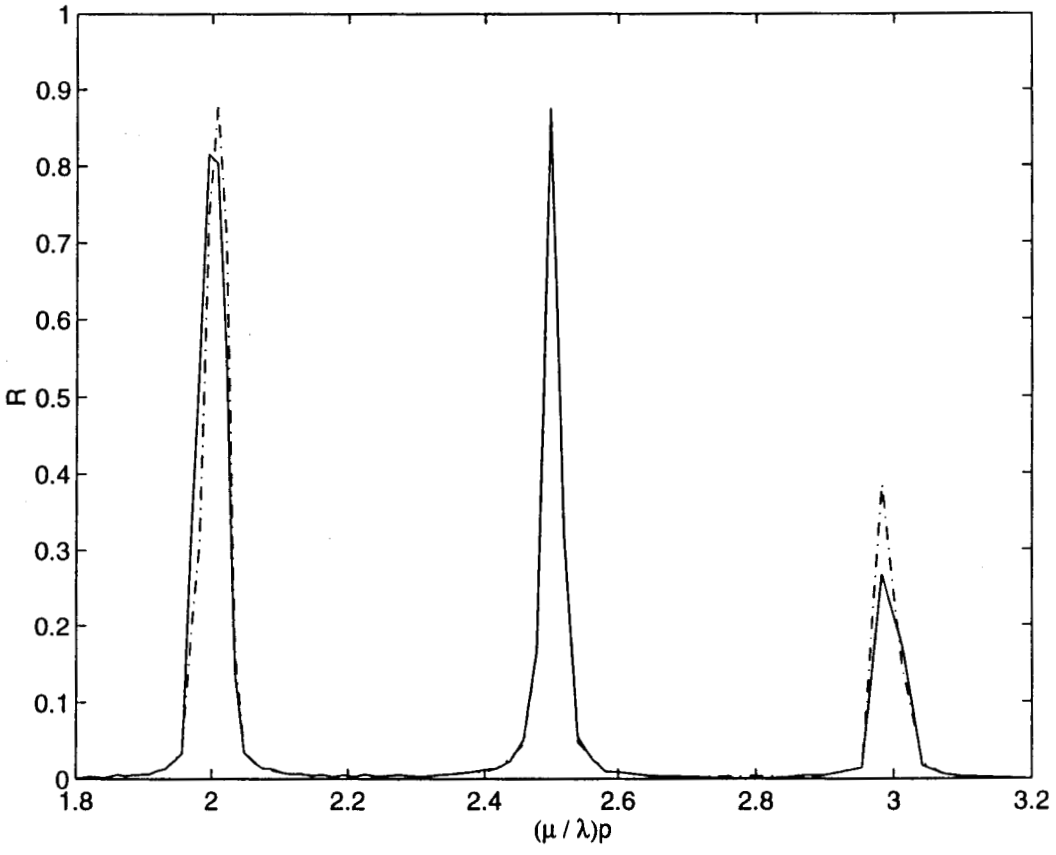

Figure 5.12: Reflection *coeffiecient* for right circularly *polarised* light. Here $R(\mathbf{k})$ is denoted by a continuous line and R(−k) is denoted by a dot-dashed line

this effect is more pronounced in reflection bands with $\mu p/\lambda = \mathrm{m}$. This is shown for some reflection bands in Figure 5.12.

Optical Rotation

Since the right and left circular light are reflected with different reflection coeffiecients from bands with integral $\mu p/\lambda$ we can think of the possibility of them acquiring different phases during the propagation. As a

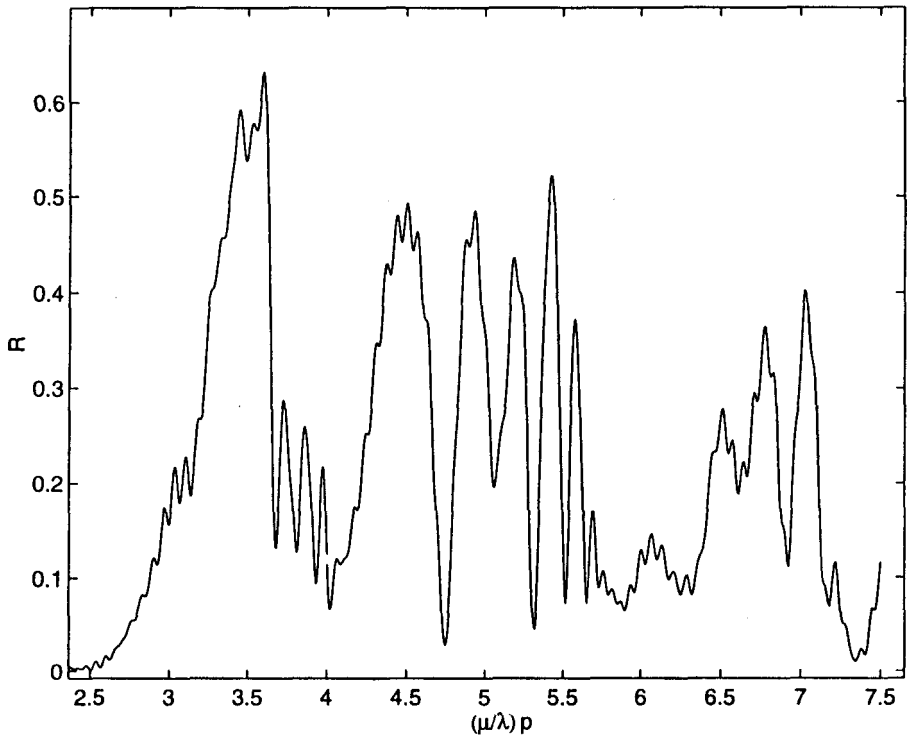

Figure 5.13: *Reflection curve for a real twist-tapered lattice for incidence of left circularly polarised light*

result, they not only show optical rotation but the rotation changes sign within a reflection band. Thus there is an *anomalous* rotation of the kind discussed in the case of TGBS. This optical rotation is absent is reflection bands of half integral $\mu p/\lambda$.

A real twist-tapered lattice

We consider now the tapered lattice permitted by the equation of motion. As said earlier its period is not constant all through. Its reflection spectrum is shown in Figure 5.13. In this case we find Every reflection band is wide with no clearly defined prominent peaks. But for this, the rest of the optical features

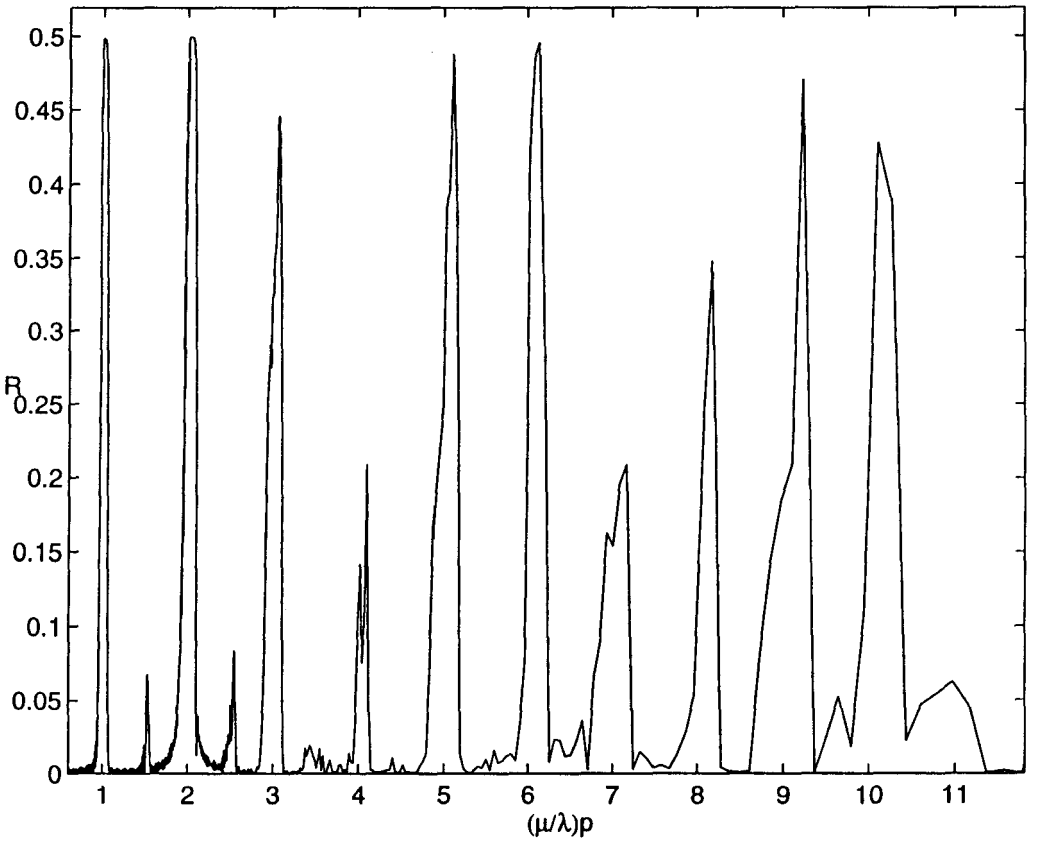

Figure 5.14: Reflection spectra for a splay-bend tapered lattice for X *polarisation.*

of the ideal case is also present in the realistic case also.

5.4.2 Splay-bend tapered lattice

In the splay-bend lattice, only for X-polarisation i.e., for electric vector in the plane of director variation the refractive index has oscillations. Hence only this polarisation experiences reflection. For the orthogonal electric vector the medium is homogenous. The prominent reflections occur at integral values of $\mu P/\lambda$. Reflections corresponding to half-integral values of $\mu P/\lambda$ are generally weak and only occur in the long wavelength regions of the spectrum. A typical

computed reflection spectra is shown in Figure 5.14.

Incidentally, in both the splay-bend and twist tapered lattices, if there was no damping and if the period of the lattice is a constant, we would get only one reflection band. This will occur at $2\mu P/\lambda = 1$ for the twist case and at $\mu P/\lambda = 1$ for the splay-bend case.

Bibliography

[1] Sunil Kumar, P.B., Ranganath, G.S., 1993 *J.Phys.II France.,* **3** 1497

[2] D. W. Berreman. , J. *Opt. Soc. Am. 62* (1972) 502

[3] P. Galatola, C. Oldano and P. B. SunilKumar . , J. *Opt. Soc. Am. A* **11** (1994) 1332

[4] L. Navailles, P. Barois and H. T. Nguyen. , *Phy. Rev. Lett.* **71** (1993) *545*

[5] A. Cottrell - *Dislocations and Plastic Flow in Crystals,* Oxford (1953)

[6] G. Srajer, R. Pindak, M. A. Waugh and J. W. Goodby ., *Phys. Rev. Lett.* 64 (1990) 1545

[7] B. D. Yanoff, A. A. Ruether, P. J. Collings, A. J. Slaney and J. W. Goodby . , *Liq. Cryst. 14* (1993) 1794

[8] V. A. Belyakov and V. E. Dmitrienko, *Soviet Scientific Reviews/Section A. 13 Part 1* Harwood Academic publishers (1989).

[9] S. Chandrasekhar and G. S. Ranganath., *Mol. Cryst. Liq. Cryst.* **25** (1974) 195

[10] G. Joly and N. Isaret, J. *Optics(Paris)* **17** (1986) 211

[11] de Vries Hl. , *Acta. Cryst.* 4 (1951) 219

[12] C. Oldano, Phys. *Rev. Lett. 53* (1984) 2413